

Measurement of Σ^- Production Polarization and Magnetic Moment

Y. W. Wah,^(a) T. R. Cardello,^(b) P. S. Cooper, L. J. Teig,^(c) and J. L. Thron^(d)
J. W. Gibbs Laboratory, Yale University, New Haven, Connecticut 06511

C. Ankenbrandt, J. P. Berge, A. E. Brenner, J. Butler, K. Doroba,^(e) J. Lach, P. Laurikainen,^(f)
 and J. Marriner
Fermi National Accelerator Laboratory, Batavia, Illinois 60510

E. McCliment
Department of Physics, University of Iowa, Iowa City, Iowa 52242

and

E. W. Anderson and A. Breakstone^(g)
Department of Physics, Iowa State University, Ames, Iowa 50011
 (Received 11 March 1985)

We have measured the production polarization of 265- and 310-GeV/ c Σ^- in the inclusive reaction $p + \text{Cu} \rightarrow \Sigma^- + X$ using 400-GeV/ c protons. The polarization was analyzed via the asymmetry in the weak decay $\Sigma^- \rightarrow n + \pi^-$, and has typical values of +0.20 with respect to the direction of the cross product of the incident-proton and Σ^- momenta. Using the spin-precession technique, we have determined the Σ^- magnetic moment to be $-1.23 \pm 0.03 \pm 0.03$ nuclear magnetons, where the statistical and systematic errors are shown separately.

PACS numbers: 14.20.Jn, 13.40.Fn, 13.85.Ni

The magnetic moments of the baryons are a useful tool for the studying of the baryons' internal structure. Recent precise measurements of baryon magnetic moments show discrepancies from the simple SU(6) quark model.¹⁻⁵ At present, theoretical models have difficulty accommodating all observed values of the baryon magnetic moments.¹ There are also currently no adequate theoretical descriptions of the mechanism producing polarized hyperons.⁶ We report the results of an experiment performed at the Fermi National Accelerator Laboratory measuring the production polarization of the Σ^- produced in the inclusive reaction $p + \text{Cu} \rightarrow \Sigma^- + X$. By observing the precession of the polarization in a magnetic field we are able to measure the Σ^- magnetic moment.

The 400-GeV/ c proton beam, shown in Fig. 1, could be steered to hit the copper target at different horizontal or vertical angles. We took data at ± 1.2 and ± 4 mrad horizontally and 0, ± 5 , and ± 7 mrad vertically at 265 GeV/ c secondary beam momentum; and 0 and ± 5 mrad vertically at 310 GeV/ c momentum. The production polarization (\mathbf{P}_Σ) is normal to the production plane. We define positive polarization to be in the $\hat{\mathbf{k}}_p \times \hat{\mathbf{k}}_\Sigma$ direction, where $\hat{\mathbf{k}}_p$ and $\hat{\mathbf{k}}_\Sigma$ are the momenta of the incident proton and the produced Σ^- , respectively.

The experimental setup is shown in Fig. 1 and has been described in detail elsewhere.⁷ For 2×10^{10} protons on the target, the secondary beam typically contained 50 000 particles per 1-s beam spill, approximately 20% of which were Σ^- . We triggered on the $\Sigma^- \rightarrow n \pi^-$ decay mode by requiring a beam track in

the proportional-wire-chamber (PWC) region, a neutral-particle signal from the neutron calorimeter, and no charged particles within the beam phase space at the downstream end of the spectrometer. Nondecaying beam tracks and pions from hyperon decay are swept by the analyzing magnets so that none could hit the neutron calorimeter. Nondecaying-beam-track calibration data were also taken, with the analyzing magnets both on and off.

The PWC tracking system measured the Σ^- momentum with resolution (σ) of 2.0 GeV/ c . The angular resolution in both dip and azimuth was 30 μrad . The position, dip, and azimuth of the π^- were measured in the drift-chamber spectrometer with resolutions (σ) of 180 μm , 30 μrad , and 100 μrad , respectively. The resulting Σ^- mass resolution of 7 MeV/ c^2 was adequate to separate Σ^- events from $\Xi^- \rightarrow \Lambda \pi^-$ background. The spectrometer had full acceptance for

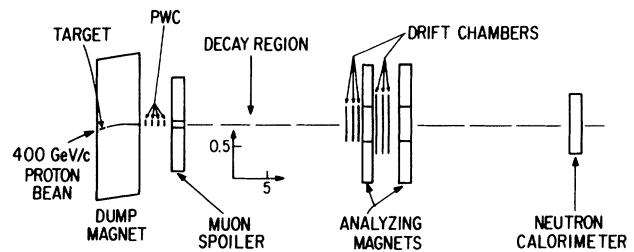


FIG. 1. Plan view of the apparatus; the scale is in meters.

the $\Sigma^- \rightarrow n\pi^-$ decay mode.

We aligned the chambers (PWC and drift chambers) with straight-through beam-track data with the analyzing magnets off. The magnetic field calibration was accomplished with beam-track data and $\Sigma^- \rightarrow n\pi^-$ triggers. Beam-track triggers (which consist mostly of noninteracting π^-) were used to adjust the ratio of the magnetic fields of the dump magnet and the analyzing magnet. The overall normalization of the fields was found by requiring that the Σ^- mass reconstructed from the $n\pi^-$ decay mode have the correct average value⁸ and be independent of the center-of-mass decay angles. The calibration was made on each run and the dump-magnet-field value had a spread of 0.3%. Similarly, the Ξ^- mass was reconstructed from the $\Lambda\pi^-$ decay mode as a crosscheck.

$\Sigma^- \rightarrow n\pi^-$ event candidates were selected by requiring good track fits in both PWC and drift-chamber systems. The PWC track was required to originate from the target and to lie within the beam phase space. The drift-chamber track was required to have momentum within the range allowed for the $\Sigma^- \rightarrow n\pi^-$ decay. Approximately 12% of the trigger events were lost in the track fitting. Another 45% of the remaining events were lost primarily as a result of target cuts and a severe longitudinal-fiducial-region cut. The upstream end of the fiducial region began 1 m downstream of the muon spoiler magnet shown in Fig. 1, so as to avoid effects due to the 100-G remnant field in the beam region.

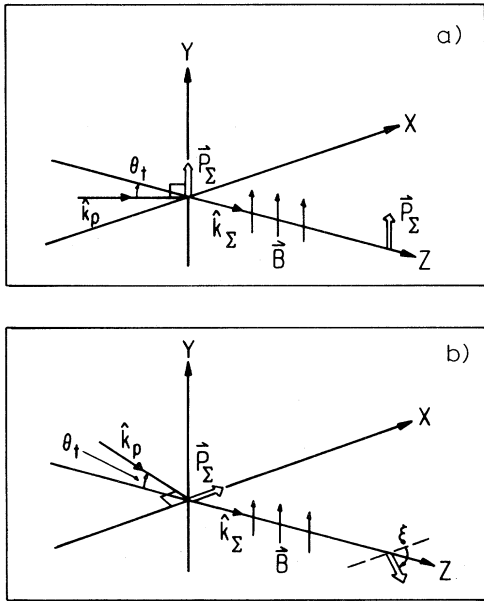


FIG. 2. The coordinate system and the vector orientations in (a) horizontal targeting and (b) vertical targeting. θ_i is the targeting angle and ξ is the precession angle measured relative to \hat{k}_Σ .

The coordinate system is shown in Fig. 2. The Y axis is vertical, the Z axis is along the direction of the Σ^- beam, and the X axis is horizontal, forming a right-handed triplet. Our sign convention for the targeting angle θ_i is given by the sign of the incident proton's momentum component transverse to the Z axis. Figure 2(a) shows a positive horizontal-targeting angle while Fig. 2(b) shows a negative vertical-targeting angle.

For horizontal targeting [shown in Fig. 2(a)] the polarization vector \mathbf{P}_Σ lies in the vertical direction parallel or antiparallel to the magnetic field \mathbf{B} . For vertical targeting [shown in Fig. 2(b)] \mathbf{P}_Σ lies in the positive or negative X direction perpendicular to the magnetic field. In either case, reversal of the targeting angle θ_i reverses the sign of the polarization. As the Σ^- moves through the magnetic field, for horizontal targeting \mathbf{P}_Σ is left unchanged; for vertical targeting \mathbf{P}_Σ precesses about the field direction by an amount proportional to the g -factor anomaly,

$$\begin{aligned} \xi &= -0.3(g/2 - 1) \int B dl / (\beta m_\Sigma c^2) \\ &= - (0.2504 \text{ rad/T-m})(g/2 - 1) \int B dl, \end{aligned} \quad (1)$$

where $\int B dl$ is the field integral of the production magnet, the minus sign is due to the negative charge of the Σ^- , and ξ is measured with respect to the Σ^- momentum vector. For the bulk of the data, $\int B dl$ was equal to -18.3 T-m, corresponding to 265 GeV/ c momentum.

The magnetic moment μ_{Σ^-} of Σ^- is related to g by

$$\mu_{\Sigma^-} = - (g/2) (m_p/m_\Sigma) \mu_N, \quad (2)$$

where m_p is the proton mass and $\mu_N = eh/2m_p c$ is the nuclear magneton.

The angle ξ can be determined from the data,

$$\xi (\text{mod } \pi) = \arctan(P_X/P_Z), \quad (3)$$

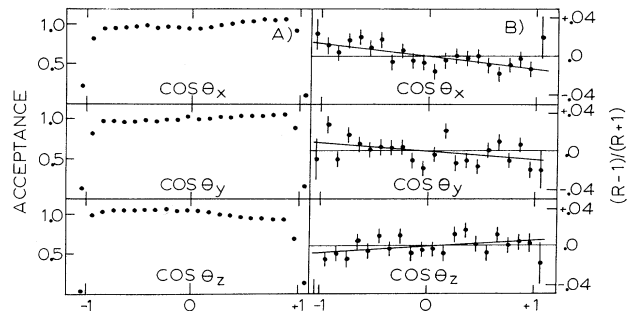


FIG. 3. (a) $A_i(\cos\theta_i)$ and (b) $\alpha_\pi P_i \cos\theta_i$ distributions for the 265-GeV/ c 5-mr vertical data set. R_i is defined as

$$\frac{dN_+/d(\cos\theta_i)}{dN_-/d(\cos\theta_i)}.$$

The acceptance is in arbitrary units.

where P_X and P_Z are the polarizations in the X and Z directions, respectively.

The center-of-mass direction cosines of the pion are calculated directly from laboratory quantities in the following manner:

$$\begin{aligned} \cos\theta_i &= p_i/p_T = p_\pi(\theta_i^\pi - \theta_i^\Sigma)/p_T, \quad i = X, Y, \\ \cos\theta_Z &= A(p_\pi/p_\Sigma) - B, \end{aligned} \quad (4)$$

where $p_T = 0.193$ GeV/ c is the center-of-mass decay momentum, p_i and θ_i are the measured momentum and angles, and A and B are constants of the $\Sigma^- \rightarrow n\pi^-$ decay kinematics. This method of calculating the direction cosines does not limit the cosines to lie within -1 and $+1$. Rather, the slopes at the

edges of the cosine plots shown in Fig. 3(a) give the resolutions in the $\cos\theta_i$. All $\cos\theta_i$ resolutions are less than 0.05.

At this stage of the analysis, a cut was made on the $\Lambda\pi^-$ reconstructed mass to eliminate Ξ^- decay events. A cut was also made to eliminate background due to straight-through tracks and interactions ($0.90 < \sum_i \cos^2\theta_i < 1.10$). These cuts reduced the event sample by approximately 10%. The remaining 6.8×10^5 events were split approximately evenly between horizontal targeting runs and vertical targeting runs. The remaining background was estimated to be less than 0.17% of the event sample.

The polarization analysis was then done by assuming the following form for the normalized distributions of the components of the center-of-mass decay angle:

$$dN_\pm/d(\cos\theta_i) = A_i(\cos\theta_i)(1 \pm \alpha_\pi P_i \cos\theta_i), \quad i = X, Y, Z, \quad (5)$$

where the subscript \pm denotes positive and negative targeting angles. The $A_i(\cos\theta_i)$ are the acceptances in $\cos\theta_i$ bins which include apparatus and analysis biases, efficiencies, etc., but not targeting-angle biases. α_π is the pion $n\pi^-$ decay asymmetry parameter⁸ which equals $+0.068 \pm 0.008$. $\alpha_\pi P_i \cos\theta_i$ and A_i are then found as follows:

$$\begin{aligned} \alpha_\pi P_i \cos\theta_i &= 0.5 \left[dN_+/d(\cos\theta_i) - dN_-/d(\cos\theta_i) \right] [A_i(\cos\theta_i)]^{-1}, \\ A_i(\cos\theta_i) &= 0.5 \left[dN_+/d(\cos\theta_i) + dN_-/d(\cos\theta_i) \right]. \end{aligned} \quad (6)$$

Shown in Fig. 3 are A_i and $\alpha_\pi P_i \cos\theta_i$ distributions for the 265-GeV/ c 5-mrad vertical data. The acceptances are high and uniform. To check for biases, the A_i distributions were compared with the acceptance of the 0-mrad data; they were found to be the same within statistics. The polarization asymmetries ($\alpha_\pi P_i$) were obtained by fitting the slopes of Fig. 3(b). These are also summarized for all data sets in Table I. The fits are shown in Fig. 3(b). This data set has the statistically largest false asymmetry that we observed (2σ in $\cos\theta_y$). This is also the only bad fit among all the data sets ($\chi^2/\nu = 2.1$). Figure 4(a) shows the total polarization of all the data calculated by summing the nonfalse polarization asymmetries and dividing by α_π [$P_\Sigma = (\alpha_\pi P_y)/\alpha_\pi$, horizontal; $P_\Sigma = \{(\alpha_\pi P_x)^2$

$+$ $(\alpha_\pi P_z)^2\}^{1/2}/\alpha_\pi$, vertical].

From the vertical-targeting-angle data, as shown in Fig. 4(b), we determined the precession angle ξ using Eq. (3). The initial-polarization-direction ambiguity was resolved by the horizontal-targeting-angle data where the spin did not precess. Since we have two different beam momenta in vertical-targeting data, in principle the remaining $2\pi n$ rotational ambiguity of the amount of precession could be removed. As a result of the statistical error of our higher-momentum data, however, we were only able to restrict the precession angle ξ to two values. Of these two values, only the one we quote below is compatible with previous published data.⁹

TABLE I. Polarization asymmetries for each of the five kinematic points at which data were taken. θ_t is the proton targeting angle and direction. $x_F = k_\Sigma/k_p$ and P_t are the Σ^- Feynman x and transverse momentum, respectively. The range of these variables is $\pm 7\%$ in x_F and ± 0.14 GeV in P_t . The italicized polarization asymmetries are false asymmetries which should be zero.

θ_t (mr)	x_F	P_t (GeV)	Events	$\alpha_\pi P_x$ (%)	$\alpha_\pi P_y$ (%)	$\alpha_\pi P_z$ (%)	P_Σ (%)
1.2 Horiz.	0.66	0.32	125×10^3	0.30 ± 0.51	-0.83 ± 0.52	0.46 ± 0.53	12 ± 8
4 Horiz.	0.66	1.06	136×10^3	-0.10 ± 0.49	-1.78 ± 0.50	0.80 ± 0.50	26 ± 7
5 Vert.	0.66	1.25	333×10^3	-1.45 ± 0.31	-0.79 ± 0.32	0.80 ± 0.31	24 ± 5
7 Vert.	0.66	1.75	33×10^3	-1.44 ± 0.96	1.24 ± 0.97	0.52 ± 0.98	23 ± 14
5 Vert.	0.78	1.50	56×10^3	-0.92 ± 0.73	-0.66 ± 0.74	0.93 ± 0.74	19 ± 11

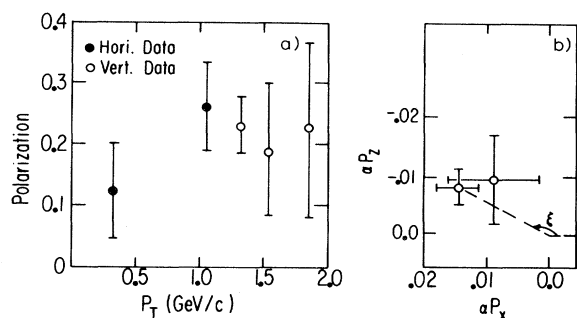


FIG. 4. (a) The total polarization and (b) the polarization components used to determine the precession angle.

The angle ξ was found to be 2.64 ± 0.19 rad for the 265-GeV data. The magnetic moment derived is then $(-1.23 \pm 0.03 \pm 0.03)\mu_N$ where the statistical and systematic errors are shown separately. Systematic studies included the effects of the remnant field in the muon spoiler magnet, possible biases due to nonexact reversal of the targeting angle, and the variation of the result as the cuts were varied. The false asymmetry in the Y direction in the magnetic-moment data set is probably associated with the spoiler field. This field, however, has a much smaller effect in the X and Z directions where the moment is measured.

Our result on the magnetic moment complements the recent precision measurement of $(-1.111 \pm 0.031 \pm 0.011)\mu_N$ done by means of the x rays from Σ^- atoms.⁵ The difference between that result and ours is 2.3 standard deviations with the quoted errors combined in quadrature. The statistical probability of such a disagreement is 2%. We see no explanation for this disagreement. Nonetheless, these two measurements, using totally different techniques, determine the Σ^- moment to the 6% level.

We are grateful to the staff of Fermilab, particularly the Proton, Physics, and Computing Departments for their assistance. This work was supported in part by

the U.S. Department of Energy under Contracts No. DE-AC-02-76-CHO-300 and No. DE-AC-02-76-ERO-3075.

(a) Present address: Enrico Fermi Institute, University of Chicago, Chicago, Ill. 60637.

(b) Present address: 15 East 11th Street, New York, N.Y. 10003.

(c) Present address: MITRE Corp., Bedford, Mass. 01730.

(d) Present address: Argonne National Laboratory, Argonne, Ill. 60439.

(e) Present address: Institute of Physics, Warsaw University, Warsaw, Poland.

(f) Present address: Department of High Energy Physics, University of Helsinki, Helsinki, Finland.

(g) Present address: Department of Physics and Astronomy, University of Hawaii, Honolulu, Haw. 96822.

¹L. G. Pondrom, in *High Energy Spin Physics—1982*, edited by Gerry M. Bunce, AIP Conference Proceedings No. 95 (American Institute of Physics, New York, 1983), pp. 45–53; A. DeRújula, H. Georgi, and S. L. Glashow, *Phys. Rev. D* **12**, 147 (1975).

²B. L. Roberts *et al.*, *Phys. Rev. D* **12**, 1232 (1975).

³G. Dugan *et al.*, *Nucl. Phys.* **A254**, 396 (1975).

⁴L. Deck *et al.*, *Phys. Rev. D* **28**, 1 (1983).

⁵D. W. Hertzog *et al.*, *Phys. Rev. Lett.* **51**, 1131 (1983).

⁶K. Heller *et al.*, *Phys. Rev. Lett.* **41**, 607 (1978); B. Anderson, G. Gustafson, and G. Ingleman, *Phys. Lett.* **85B**, 417 (1979); T. A. Degrand and H. I. Miettinen, *Phys. Rev. D* **24**, 2419 (1981).

⁷C. Ankenbrandt *et al.*, *Phys. Rev. Lett.* **51**, 863 (1983); T. Cardello, Fermilab Report No. TM-964, 1984 (unpublished); Y. Wah, thesis, Yale University, 1983 (unpublished).

⁸C. G. Wohl *et al.*, *Rev. Mod. Phys.* **56**, S1 (1984). Note that this reference quotes the neutron asymmetry for the $n\pi^-$ decay mode which is $-\alpha_\pi$.

⁹The other value of the precession angle was $\xi = -3.64 \pm 0.19$ rad, giving a magnetic moment of $(-0.16 \pm 0.03)\mu_N$ in gross disagreement with Ref. 5.